

# Effects of Extrinsic Proteins on the Protein Conformation of the Oxygen-Evolving Center in Cyanobacterial Photosystem II As Revealed by Fourier Transform Infrared Spectroscopy

Ryo Nagao,<sup>\*,†</sup> Tatsuya Tomo,<sup>‡,§</sup> and Takumi Noguchi<sup>\*,†</sup>

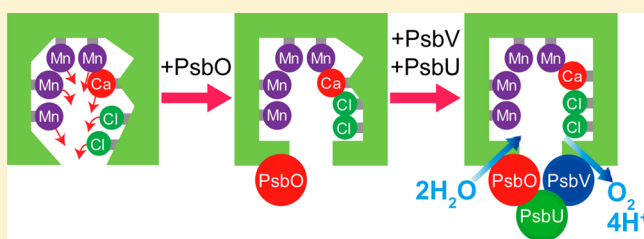
<sup>†</sup>Division of Material Science, Graduate School of Science, Nagoya University, Furo-cho, Chikusa-ku, Nagoya 464-8602, Japan

<sup>‡</sup>Department of Biology, Faculty of Science, Tokyo University of Science, Kagurazaka 1-3, Shinjuku-ku, Tokyo 162-8601, Japan

<sup>§</sup>PRESTO, Japan Science and Technology Agency (JST), Saitama 332-0012, Japan

## Supporting Information

**ABSTRACT:** Extrinsic proteins of photosystem II (PSII) play an important role in optimizing oxygen-evolving reactions in all oxyphototrophs. The currently available crystal structures of cyanobacterial PSII core complexes show the binding structures of the extrinsic proteins, PsbO, PsbV, and PsbU; however, how the individual extrinsic proteins affect the structure and the function of the oxygen-evolving center (OEC) in cyanobacterial PSII remains unknown. In this study, we have investigated the effects of the binding of the extrinsic proteins on the protein conformation of the OEC in PSII core complexes from the thermophilic cyanobacterium *Thermosynechococcus elongatus*, using light-induced Fourier transform infrared (FTIR) difference spectroscopy. Upon removal of the three extrinsic proteins, an  $S_2$ -minus- $S_1$  FTIR difference spectrum measured in the presence of a high  $\text{CaCl}_2$  concentration showed a drastic change in amide I bands, reflecting perturbation of the secondary structures of polypeptides, whereas the overall spectral intensity was lost at a low  $\text{CaCl}_2$  concentration, indicative of inactivation of the  $\text{Mn}_4\text{CaO}_5$  cluster. The amide I features as well as the overall intensity were recovered mainly by binding of PsbO, while complete amide I recovery was achieved by further binding of PsbV and PsbU. We thus concluded that PsbO, together with smaller contributions of PsbV and PsbU, plays a role in the maintenance of the proper protein conformation of the OEC in cyanobacterial PSII, which provides the stability of the  $\text{Mn}_4\text{CaO}_5$  cluster via the enhanced retention capability of  $\text{Ca}^{2+}$  and  $\text{Cl}^-$  ions.



Photosystem II (PSII) is a multisubunit pigment–protein complex catalyzing light-driven water oxidation in plants and cyanobacteria.<sup>1–6</sup> The active site of water oxidation is the oxygen-evolving center (OEC), which consists of the  $\text{Mn}_4\text{CaO}_5$  cluster, two chloride ions located  $\sim 7$  Å from the nearest Mn ions, and surrounding amino acid residues.<sup>7–10</sup> Water oxidation is performed by a cycle of five intermediates designated  $S_n$  states ( $n = 0–4$ ).<sup>1–6</sup> The  $S_1$  state predominates in the dark, and flash illumination advances the  $S_n$  state to the  $S_{n+1}$  state ( $n = 0–3$ ). The  $S_4$  state is a transient intermediate and immediately relaxes to the  $S_0$  state after releasing  $\text{O}_2$ .

PSII complexes consist of membrane-spanning intrinsic proteins and several extrinsic proteins bound on the luminal surface.<sup>7–10</sup> The intrinsic proteins are well-conserved among oxyphototrophs, whereas the composition of extrinsic proteins in PSII complexes is rather different depending on species except for the PsbO protein, which is commonly involved in PSII.<sup>11–16</sup> Cyanobacteria, which are thought to be an ancestor of chloroplasts in both red and green lineages,<sup>17</sup> have extrinsic proteins PsbO, PsbV, and PsbU.<sup>9,18,19</sup> In addition, CyanoP and CyanoQ are involved in or functionally related to PSII in cyanobacteria,<sup>20–22</sup> although these two proteins have not been found in the X-ray crystal structure of PSII core complexes

from *Thermosynechococcus elongatus* and *Thermosynechococcus vulcanus*.<sup>7–10</sup> In the red lineage, red algae have PsbO, PsbV, PsbU, and PsbQ,<sup>23,24</sup> while diatoms have PsbO, PsbV, PsbU, PsbQ', and Psb31.<sup>25–28</sup> In the green lineage, on the other hand, both green algae and higher plants have PsbO, PsbP, and PsbQ but with different binding topologies.<sup>29,30</sup> The origins of PsbP and PsbQ are thought to be CyanoP and CyanoQ, respectively, in cyanobacteria, although their functions in OEC are significantly different.<sup>20,31</sup> Thus, PsbV and PsbU are conserved in cyanobacteria and the red lineage, whereas they were lost in the green lineage; instead, PsbP and PsbQ were developed.

The major role of extrinsic proteins of PSII is regulation of oxygen-evolving reactions via stabilization of the  $\text{Mn}_4\text{CaO}_5$  cluster and  $\text{Cl}^-$  ions.<sup>12,13,16</sup> However, in the X-ray crystallographic structures of PSII from thermophilic cyanobacteria (Figure 1), the extrinsic proteins directly interact with neither the  $\text{Mn}_4\text{CaO}_5$  cluster nor the  $\text{Cl}^-$  ions.<sup>7–10</sup> Thus, it is presumed that binding of the extrinsic proteins on the luminal side of PSII intrinsic proteins influences the protein structure around

Received: January 20, 2015

Revised: March 5, 2015

Published: March 6, 2015



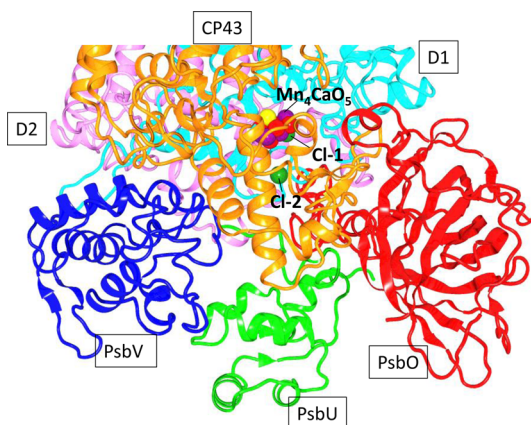


**Figure 1.** Localization of the extrinsic proteins on the luminal side of the PSII core complex of a thermophilic cyanobacterium. The structure was deduced from the high-resolution (1.9 Å) X-ray crystallographic structure of *T. vulcanus* (Protein Data Bank entry 3ARC<sup>9</sup>). Only the D1 (cyan), D2 (pink), and CP43 (orange) proteins are shown as intrinsic proteins, together with the PsbO (red), PsbV (blue), and PsbU (green) extrinsic proteins.

the OEC, resulting in the change in the stability of the  $\text{Mn}_4\text{CaO}_5$  cluster and  $\text{Cl}^-$  ions.<sup>12,13,16</sup> However, the molecular mechanism of how the interactions of individual extrinsic proteins affect the OEC structure in achieving its stability remains to be clarified.

Light-induced Fourier transform infrared (FTIR) difference spectroscopy is a powerful tool for detecting the structural changes in the OEC in the S-state transitions, including the changes in the secondary structures of polypeptide main chains, amino acid side chains, and hydrogen bond networks of proteins and water molecules.<sup>32–41</sup> Using this technique, we have previously investigated the effect of the binding of extrinsic proteins on the protein conformation of OEC in spinach PSII membranes and PSII core complexes from the red alga *Cyanidium caldarium*.<sup>42–46</sup> It was shown that amide I bands in  $\text{S}_2$ -minus- $\text{S}_1$  difference spectra, which represent the changes in the protein conformations of the OEC during the  $\text{S}_1 \rightarrow \text{S}_2$  transition, were retained mainly by binding of PsbP and PsbV in spinach and *C. caldarium*, respectively. These results suggest the significance of PsbP and PsbV in maintaining the proper protein conformation of the OEC, which should be related to the  $\text{O}_2$  evolution activity and the  $\text{Ca}^{2+}$  and  $\text{Cl}^-$  retention capability, while PsbO is required for functional binding of these proteins as well as stabilization of the  $\text{Mn}_4\text{CaO}_5$  cluster. These FTIR observations, however, raise a new question of which extrinsic protein, PsbO, PsbV, or PsbU, regulates the OEC conformation in cyanobacteria that are the common ancestors of plants and red algae.

In this study, we have investigated the effect of extrinsic proteins on the OEC conformation in cyanobacterial PSII by means of light-induced FTIR difference spectroscopy. We used PSII core complexes isolated from *T. elongatus*, which has PsbO, PsbV, and PsbU as extrinsic proteins. All the extrinsic proteins were first removed from the core complexes, and then the complexes were reconstituted with the extrinsic proteins with various combinations. FTIR difference spectra upon the  $\text{S}_1 \rightarrow \text{S}_2$  transition were measured, and the effects of individual extrinsic proteins were examined. The obtained FTIR results were compared with the previous FTIR data of spinach and red

algae to provide insight into the evolution of extrinsic proteins of PSII in light of their functions.

## MATERIALS AND METHODS

**Isolation of  $\text{O}_2$ -Evolving PSII Core Complexes.**  $\text{O}_2$ -evolving PSII core complexes from the *T. elongatus* 47-H strain, in which a six-histidine tag was introduced onto the carboxyl terminus of the CP47 subunit,<sup>47</sup> were purified using  $\text{Ni}^{2+}$  affinity column chromatography following the previously described method<sup>48</sup> with slight modifications. The PSII core complexes eluted from the affinity column were precipitated by centrifugation at 48000g for 20 min after addition of 10% (w/v) polyethylene glycol 6000 (PEG6000) and subsequently suspended in a buffer containing 40 mM Mes-NaOH (pH 6.5), 10 mM  $\text{CaCl}_2$ , 10 mM  $\text{MgCl}_2$ , 10% glycerol, and 1 M betaine. The  $\text{O}_2$  evolution activity of the obtained PSII core complexes was 2000–2500  $\mu\text{mol}$  of  $\text{O}_2$  (mg of chlorophyll)<sup>−1</sup> h<sup>−1</sup> at 25 °C in the presence of 0.5 mM 2,6-dichloro-1,4-benzoquinone as an electron acceptor. The PSII core complexes were stored in liquid nitrogen until they were used.

**Purification of Extrinsic Proteins.** The three extrinsic proteins, PsbO, PsbV, and PsbU, were extracted from the PSII core complexes of *T. elongatus* and purified following the method of Shen and Inoue<sup>18</sup> with some modifications. The purified PSII core complexes were treated with 1 M  $\text{CaCl}_2$ , and a supernatant after centrifugation of the sample in the presence of 10% PEG6000 was dialyzed against 20 mM Mes-NaOH buffer (pH 6.5). The dialyzed samples were applied to a DEAE Toyopearl 650 M column (Tosoh) equilibrated with 20 mM Mes-NaOH (pH 6.5). PsbO was first eluted at 100 mM NaCl, followed by fractionation of PsbV and PsbU. The fraction containing PsbV and PsbU was dialyzed in 20 mM citric acid/NaOH buffer (pH 4.0). The dialyzed samples were applied to a CM Toyopearl 650 M column (Tosoh) equilibrated with 20 mM citric acid/NaOH buffer (pH 4.0). PsbU and then PsbV were eluted at 100 mM NaCl. The three extrinsic proteins were dialyzed in 20 mM Mes-NaOH buffer (pH 6.5) and concentrated by ultrafiltration using a 10 kDa cutoff filter (Amicon Ultra, Millipore). Successful purification of the extrinsic proteins was confirmed by sodium dodecyl sulfate–polyacrylamide gel electrophoresis (SDS–PAGE) (Figure S1 of the Supporting Information). The three extrinsic proteins were stored at −80 °C until they were used.

**Reconstitution of PSII Complexes with Extrinsic Proteins.** The PSII core complexes were depleted of the three extrinsic proteins by treatment with 1 M  $\text{CaCl}_2$  for 30 min on ice in the dark. After centrifugation at 16000g for 10 min in the presence of 10% PEG6000, the precipitate was suspended in a buffer containing 10 mM Mes-NaOH (pH 6.0), 5 mM NaCl, 5 mM  $\text{CaCl}_2$ , and 25% glycerol. The thus obtained PSII complexes were mixed with the extrinsic proteins at a molar ratio of 3:1 (for each extrinsic protein) with respect to a PSII reaction center. The sample was incubated for 30 min on ice in the dark and then collected by centrifugation in the presence of 10% PEG6000. Reconstituted samples were prepared just before FTIR measurements.

**SDS–PAGE Analysis of PSII Samples after FTIR Measurements.** Samples after FTIR measurements were suspended in 40 mM Mes-NaOH buffer (pH 6.0) containing 0.4 M sucrose and solubilized with 3% lithium lauryl sulfate in the presence of 75 mM dithiothreitol, followed by incubation for 30 min at room temperature. The solubilized PSII samples (2  $\mu\text{g}$  of chlorophyll) were subjected to SDS–PAGE using a

16% acrylamide gel containing 7.5 M urea. A standard molecular weight marker (Prestained XL-Ladder, APRO Life Science Institute) was used. After electrophoresis, the gels were stained with Coomassie Brilliant Blue R-250 and photographed.

**FTIR Measurements.** For FTIR measurements, PSII complexes (corresponding to 100  $\mu\text{g}$  of chlorophyll) were suspended in a buffer containing 10 mM MES-NaOH (pH 6.0), 5 mM NaCl, and either 5 or 100 mM  $\text{CaCl}_2$  in the presence of 30 mM potassium ferrocyanide and 20 mM potassium ferricyanide at a chlorophyll concentration of 0.05  $\text{mg mL}^{-1}$  and then precipitated at 170000g for 15 min in the presence of 10% PEG6000. The resultant pellet was sandwiched between two  $\text{CaF}_2$  plates (25 mm in diameter). Ferricyanide acts as an exogenous electron acceptor and ferrocyanide maintains the redox potential of the medium relatively low to keep the non-heme iron in the reduced form.<sup>49</sup> One of the  $\text{CaF}_2$  plates has a circular groove (14 mm inner diameter, 1 mm width), and the sample cell was sealed with silicone grease laid on the outer part of the groove. A piece of aluminum foil ( $\sim 1 \text{ mm} \times \sim 1 \text{ mm}$ ;  $\sim 15 \mu\text{m}$  thickness) was placed as a spacer in the outer part of the cell.<sup>50</sup> The sample temperature was adjusted to 10  $^\circ\text{C}$  by circulating cold water in a copper holder. The sample was stabilized at this temperature in the dark for more than 2 h before the spectra were recorded.

Flash-induced  $\text{S}_2/\text{S}_1$  FTIR difference spectra were recorded using a Bruker IFS-66/S spectrophotometer equipped with an MCT detector (InfraRed D313-L) at 4  $\text{cm}^{-1}$  resolution. Illumination of flashes was performed by a Q-switched Nd:YAG laser (Quanta-Ray GCR-130; 532 nm,  $\sim 7 \text{ ns}$  full width at half-maximum) with a power of  $\sim 7 \text{ mJ pulse}^{-1} \text{ cm}^{-2}$  at the sample point. The sample was subjected to two preflashes (1 Hz) followed by dark relaxation to synchronize all centers to the  $\text{S}_1$  state, reduce the preoxidized non-heme iron to  $\text{Fe}^{2+}$ , and oxidize  $\text{Y}_D$ . A single-beam spectrum (10 s scans) was recorded twice before and once after the illumination of a single flash. The measurement was repeated 80 times with a dark interval of 10 and 12.5 min for samples (control, +PsbO, +PsbO/V, and +PsbO/V/U) in the presence of 5 and 100 mM  $\text{CaCl}_2$ , respectively. For samples in which all the extrinsic proteins were depleted and only PsbV was rebound, a dark interval of 2.5 min was adopted because of much shorter relaxation times (15–25 s in comparison with 70–110 s in the control sample). The averaged spectra were used to calculate an  $\text{S}_2/\text{S}_1$  FTIR difference spectrum as after-minus-before illumination. A difference spectrum between the two spectra before illumination represents a baseline and a noise level. After FTIR measurements, PSII samples were retrieved from the  $\text{CaF}_2$  plates and subjected to SDS–PAGE to confirm the intended composition of the extrinsic proteins in the PSII core complexes (Figure 2).

Spectral fitting was performed using Igor Pro (WaveMetrics Inc.). The spectra of treated PSII samples were normalized to that of the untreated PSII with factors determined by the fitting in the 1450–1350  $\text{cm}^{-1}$  region (symmetric  $\text{COO}^-$  stretching vibrations).<sup>45</sup> Double-difference spectra were calculated by subtracting the normalized spectra from the spectrum of the untreated PSII.

## RESULTS

Figure 3a (black line) shows a light-induced  $\text{S}_2$ -minus- $\text{S}_1$  (designated  $\text{S}_2/\text{S}_1$ ) FTIR difference spectrum of the PSII core complexes from *T. elongatus* in the presence of a relatively low concentration of  $\text{CaCl}_2$  (5 mM). The spectrum is virtually

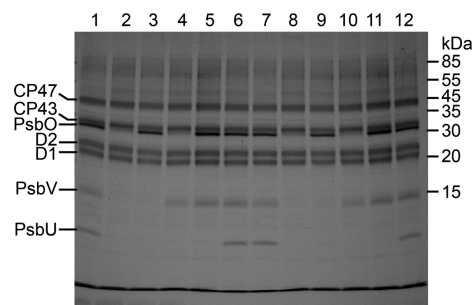


**Figure 2.** SDS–PAGE analysis of the PSII samples after FTIR measurements in the presence of 5 mM  $\text{CaCl}_2$  (lanes 1–6) and 100 mM  $\text{CaCl}_2$  (lanes 7–12): lanes 1 and 7, untreated PSII; lanes 2 and 8, PSII depleted of all the extrinsic proteins; lanes 3 and 9, PsbO-reconstituted PSII; lanes 4 and 10, PsbV-reconstituted PSII; lanes 5 and 11, PsbO/V-reconstituted PSII; lanes 6 and 12, PsbO/V/U-reconstituted PSII.

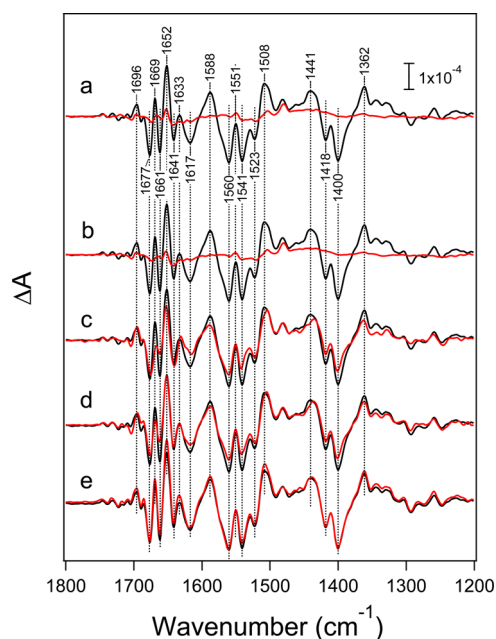


**Figure 3.**  $\text{S}_2$ -minus- $\text{S}_1$  FTIR difference spectra of PSII core complexes from *T. elongatus* in the presence of a low concentration of  $\text{CaCl}_2$  (5 mM). PSII core complexes were depleted of all the extrinsic proteins (a) and then reconstituted with PsbV (b), PsbO (c), PsbO/V (d), and PsbO/V/U (e). Each spectrum of the treated PSII samples (red lines) is compared with the spectrum of the untreated PSII (black line). The intensities of the spectra were normalized on the basis of the absorbance of an amide II band at 1549  $\text{cm}^{-1}$  in original FTIR spectra before taking a difference.

identical to the  $\text{S}_2/\text{S}_1$  FTIR spectra of PSII core complexes from *T. elongatus* reported previously.<sup>51–54</sup> Prominent bands were observed at 1700–1600 and 1600–1500  $\text{cm}^{-1}$  in the amide I (CO stretching vibrations of backbone amides) and amide II (NH bending and CN stretching vibrations of backbone amides) regions, respectively, representing the changes in the secondary structures of polypeptide chains around the  $\text{Mn}_4\text{CaO}_5$  cluster.<sup>55,56</sup> Characteristic bands also appeared at 1450–1350  $\text{cm}^{-1}$  arising from the symmetric  $\text{COO}^-$  stretching vibrations, while the coupled asymmetric  $\text{COO}^-$  stretching bands overlap the amide II region at 1600–1500  $\text{cm}^{-1}$ .<sup>55,56</sup> These  $\text{COO}^-$  bands are attributed to the

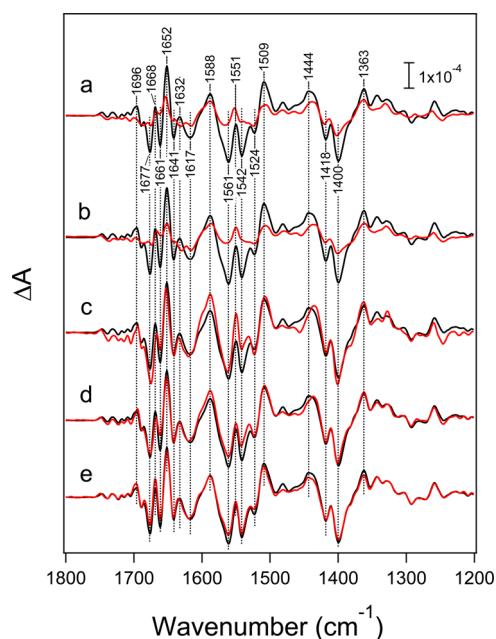
changes in the interactions of carboxylate residues around the  $\text{Mn}_4\text{CaO}_5$  cluster.<sup>35,36,57–60</sup>

The PSII complexes were depleted of all the extrinsic proteins and then reconstituted with various combinations of extrinsic proteins.  $S_2/S_1$  FTIR difference spectra of these treated PSII samples, measured in the presence of 5 mM  $\text{CaCl}_2$ , are also shown in Figure 3 (red lines) in comparison with the control spectrum of untreated PSII (black lines). The spectra were normalized on the basis of the amount of protein, which was estimated by the intensity of an amide II band at  $1549\text{ cm}^{-1}$  in original FTIR absorption spectra before taking a difference. When all the extrinsic proteins were removed, the overall spectral intensity was lost (Figure 3a, red line), indicating the inactivation of the  $\text{Mn}_4\text{CaO}_5$  cluster.

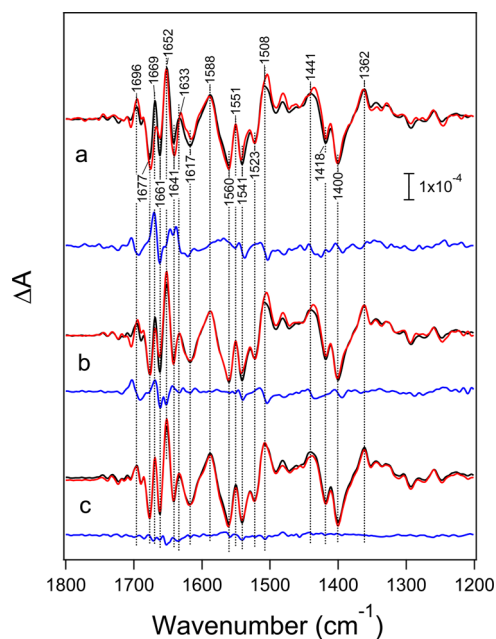
It has been reported that in cyanobacterial PSII complexes, PsbO and PsbV each independently bind to the intrinsic proteins, whereas PsbU requires the presence of both PsbO and PsbV for its binding to PSII.<sup>18,61</sup> The spectral intensity was not recovered by binding of PsbV (Figure 3b, red line), indicating that the sole binding of PsbV is not effective for maintaining the  $\text{Mn}_4\text{CaO}_5$  cluster at a low  $\text{CaCl}_2$  concentration. The situation drastically changed when PsbO was bound and the spectral intensity was mostly recovered (Figure 3c, red line). The spectral features are also very similar to those of the control spectrum, except that peaks at  $1669(+)/1661(-)\text{ cm}^{-1}$  in the amide I region are clearly lost in the PsbO-reconstituted sample. The spectral intensity and the  $1669/1661\text{ cm}^{-1}$  peaks were further recovered upon binding of PsbO and PsbV [expressed as PsbO/V (Figure 3d, red line)], while simultaneous binding of all the three PsbO/V/U proteins fully recovered the control spectrum (Figure 3e, red line).

Figure 4 shows  $S_2/S_1$  FTIR difference spectra of the untreated and treated PSII samples (black and red lines, respectively) measured in the presence of 100 mM  $\text{CaCl}_2$ . The spectra were normalized on the basis of the amount of protein as in Figure 3. The spectral features of the untreated PSII (black lines) were virtually identical to those with 5 mM  $\text{CaCl}_2$  (Figure 3, black lines). In contrast to the case of 5 mM  $\text{CaCl}_2$ , with 100 mM  $\text{CaCl}_2$ , the spectra of PSII depleted of all the extrinsic proteins (Figure 4a, red line) and reconstituted with PsbV (Figure 4b, red line) recovered their overall intensities by  $\sim 50\%$ , although the structures in the amide I region were less recovered. The spectral intensities were fully recovered by reconstitution with PsbO, PsbO/V, and PsbO/V/U (spectra c, d, and e of Figure 4, respectively, red lines), judging from the symmetric  $\text{COO}^-$  stretching region ( $1450\text{--}1350\text{ cm}^{-1}$ ). However, in the samples reconstituted with PsbO and with PsbO/V, the peaks at  $1668/1661\text{ cm}^{-1}$  in the amide I region were still not fully recovered.

Because the spectral features in the symmetric  $\text{COO}^-$  stretching region of the treated PSII samples (except for the all-depleted and PsbV-reconstituted PSII samples with 5 mM  $\text{CaCl}_2$ ) were virtually identical to those of the untreated PSII (Figures 3 and 4), the intensities of the  $S_2/S_1$  spectra of the treated PSII were normalized to the control spectrum based on the intensities of this  $\text{COO}^-$  region ( $1450\text{--}1350\text{ cm}^{-1}$ ). The factors for normalization were determined by least-squares fitting of the spectra in this region. Figures 5 and 6 (red lines) show the resultant normalized spectra with 5 and 100 mM  $\text{CaCl}_2$ , respectively, in comparison with the corresponding control spectrum (black lines) of the untreated PSII. Spectra of the all-depleted and PsbV-reconstituted PSII samples with 5 mM  $\text{CaCl}_2$  are not included in Figure 5 because of the absence



**Figure 4.**  $S_2$ -minus- $S_1$  FTIR difference spectra of PSII core complexes from *T. elongatus* in the presence of a high concentration of  $\text{CaCl}_2$  (100 mM). PSII core complexes were depleted of all the extrinsic proteins (a) and then reconstituted with PsbV (b), PsbO (c), PsbO/V (d), and PsbO/V/U (e). Each spectrum of the treated PSII samples (red lines) is compared with the spectrum of the untreated PSII (black line). The intensities of the spectra were normalized on the basis of the absorbance of an amide II band at  $1549\text{ cm}^{-1}$  in original FTIR spectra before taking a difference.



**Figure 5.**  $S_2$ -minus- $S_1$  FTIR difference spectra of untreated (black lines) and treated (red lines) PSII core complexes in the presence of a low concentration of  $\text{CaCl}_2$  (5 mM) normalized at the symmetric  $\text{COO}^-$  bands in the  $1450\text{--}1350\text{ cm}^{-1}$  region, and their double-difference spectra (untreated-minus-treated PSII: blue lines). PSII core complexes were reconstituted with PsbO (a), PsbO/V (b), and PsbO/V/U (c).

of the overall intensities (Figure 3a,b, red lines). Comparison of the normalized spectra of the treated and untreated samples

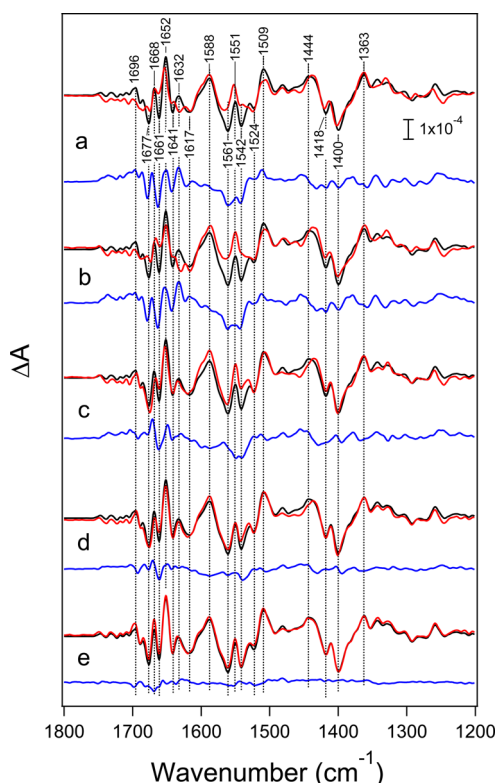


**Figure 6.**  $S_2$ -minus- $S_1$  FTIR difference spectra of untreated (black lines) and treated (red lines) PSII complexes in the presence of a high concentration  $\text{CaCl}_2$  (100 mM) normalized at the  $\text{COO}^-$  bands in the  $1450\text{--}1350\text{ cm}^{-1}$  region, and their double-difference spectra (untreated-minus-treated PSII: blue lines). PSII core complexes depleted of all the extrinsic proteins (a) were reconstituted with PsbV (b), PsbO (c), PsbO/V (d), and PsbO/V/U (e).

confirmed a high similarity in the symmetric  $\text{COO}^-$  region, whereas the spectra in the amide I region ( $1700\text{--}1600\text{ cm}^{-1}$ ) showed significant differences depending on the treatments.

To examine the spectral differences in more detail, double-difference spectra of the normalized spectra of the treated and untreated samples (untreated-minus-treated) were calculated (Figures 5 and 6, blue lines).<sup>45</sup> Several peaks are clearly observed in the amide I region ( $1700\text{--}1600\text{ cm}^{-1}$ ) in most of the samples, whereas more minor peaks or broad features are seen in the symmetric  $\text{COO}^-$  stretching ( $1450\text{--}1350\text{ cm}^{-1}$ ) and asymmetric  $\text{COO}^-$  stretching/amide II ( $1600\text{--}1500\text{ cm}^{-1}$ ) regions. The broad feature at  $1600\text{--}1500\text{ cm}^{-1}$  in spectra a–c of Figure 6 (blue lines) could be due to a baseline change, although its origin is unknown at present.

The amide I region, which reflects perturbations in the secondary structures of polypeptide backbones, of the double-difference spectra is expanded in Figure 7, in which the spectra with 5 mM  $\text{CaCl}_2$  (black lines) and 100 mM  $\text{CaCl}_2$  (red lines) are compared. The PSII complexes depleted of all the extrinsic proteins (Figure 7a) and reconstituted with PsbV (Figure 7b) in the presence of 100 mM  $\text{CaCl}_2$  showed similar large signals at  $1679(-)/1672(+)/1663(-)/1651(+)/1643(-)/1633(+)\text{ cm}^{-1}$ . In PsbO-reconstituted PSII, most of the bands disappeared and only bands at  $1671\text{--}1670(+)/1662(-)/1649\text{--}1647(+)\text{ cm}^{-1}$  were left (Figure 7c), while upon PsbO and PsbV reconstitution, the higher-frequency peaks were left at  $1671\text{--}1669(+)/1661(-)\text{ cm}^{-1}$  but with lower intensities (Figure 7d). These peaks in spectra c and d of Figure 7 were

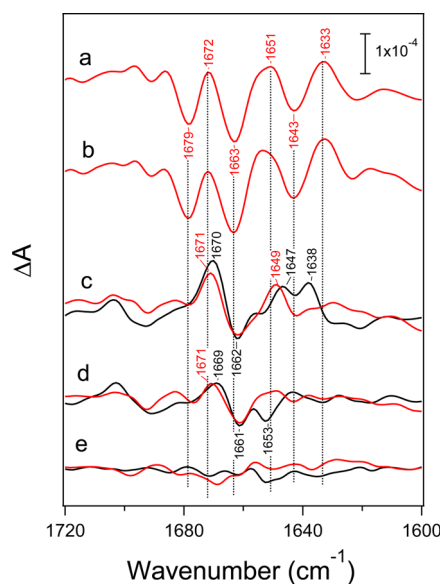


**Figure 7.** Amide I region of the double-difference (untreated-minus-treated) spectra in the presence of 5 mM  $\text{CaCl}_2$  (black lines) and 100 mM  $\text{CaCl}_2$  (red lines). PSII core complexes depleted of all the extrinsic proteins (a) were reconstituted with PsbV (b), PsbO (c), PsbO/V (d), and PsbO/V/U (e).

commonly observed at both  $\text{CaCl}_2$  concentrations of 5 and 100 mM. With 5 mM  $\text{CaCl}_2$ , an additional band was left at  $1638$  and  $1653\text{ cm}^{-1}$  in PsbO-reconstituted and PsbO/V-reconstituted PSII, respectively (spectra c and d of Figure 7, respectively, black lines). In the PsbO/V/U-reconstituted PSII, all the peaks disappeared in the double-difference spectra (Figure 7e), consistent with the full recovery of the amide I bands in the  $S_2/S_1$  difference spectra (Figures 5c and 6e).

## DISCUSSION

In this study, we examined the effect of the binding of the extrinsic proteins, PsbO, PsbV, and PsbU, on the protein conformation of OEC as well as its stability in the PSII core complexes from the cyanobacterium *T. elongatus* by means of FTIR difference spectroscopy. With a relatively low  $\text{CaCl}_2$  concentration (5 mM), the PSII complexes depleted of all the extrinsic proteins lost the spectral intensity of the  $S_2/S_1$  FTIR difference spectrum (Figure 3a), indicating that the  $\text{Mn}_4\text{CaO}_5$  cluster was inactivated under this condition. With a high  $\text{CaCl}_2$  concentration (100 mM), however, the overall intensity of the spectrum, particularly in the symmetric  $\text{COO}^-$  region, was recovered by approximately half even without any extrinsic proteins (Figure 4a). These results provide evidence of the functions of extrinsic proteins as enhancing the  $\text{Ca}^{2+}$  and  $\text{Cl}^-$  retention capability.<sup>12,13,16</sup> These FTIR data are also consistent with the observation that the  $\text{O}_2$  evolution activity of the PSII core complexes depleted of all the extrinsic proteins is higher in the presence of 100 mM  $\text{CaCl}_2$  than in the presence of 5 mM  $\text{CaCl}_2$  (27 and 10% of the activity of untreated PSII, respectively). The previous study also demonstrated that cyanobacterial PSII core complexes without the extrinsic proteins showed no  $\text{O}_2$  evolution activity in the absence of  $\text{CaCl}_2$  but showed a low activity (11% of the activity of untreated PSII) in the presence of 10 mM  $\text{CaCl}_2$ .<sup>18</sup> The effect of  $\text{CaCl}_2$  on the  $\text{O}_2$  evolution activity was slightly weaker than that on the FTIR signal probably because the FTIR measurement detects only the  $S_1 \rightarrow S_2$  transition, whereas  $\text{O}_2$

evolution activity reflects the efficiency of the whole S-state cycle. The recovery of FTIR signals and  $O_2$  evolution by high-concentration  $CaCl_2$  suggests that the OEC structures are partially retained in the presence of  $Ca^{2+}$  and  $Cl^-$  ions even in the absence of all the extrinsic proteins.

Depletion of all the extrinsic proteins also induced significant changes in the protein conformation around the  $Mn_4CaO_5$  cluster, which was monitored by the amide I bands in the  $S_2/S_1$  FTIR difference spectra measured at a high (100 mM)  $CaCl_2$  concentration (Figures 6a and 7a). The double-difference spectrum between the all-depleted and untreated PSII samples (Figure 7a) showed several peaks at 1679/1672/1663/1651/1643/1633  $cm^{-1}$  over the whole amide I region of 1700–1600  $cm^{-1}$ , indicating that several polypeptide chains with different secondary structures are affected by depletion of the extrinsic proteins. These changes arise from the disappearance or decrease in intensity of the peaks at 1677/1668/1661/1652/1641/1632  $cm^{-1}$  in the control  $S_2/S_1$  difference spectrum (Figure 6a). This suggests that the structural changes in the polypeptide chains around the  $Mn_4CaO_5$  cluster in the  $S_1 \rightarrow S_2$  transition are suppressed by depletion of the extrinsic proteins. Alternatively, the protein structures around the  $Mn_4CaO_5$  cluster could be loosened in the absence of extrinsic proteins, which induced the broadening of the amide I bands and diminished the peak intensities in the difference spectra.

The observations of instability of the  $Mn_4CaO_5$  cluster at a lower  $CaCl_2$  concentration (Figures 3b and 4b) and significant conformational changes around the  $Mn_4CaO_5$  cluster (Figures 6b and 7b) were unchanged by the single binding of PsbV, indicating that PsbV solely is not effective for the structure of OEC. In contrast to PsbV, single binding of PsbO dramatically recovered the stability of the  $Mn_4CaO_5$  cluster (Figures 3c and 4c) and the protein conformation of OEC (Figures 5a, 6c, and 7c). This is consistent with the previous observations that rebinding of PsbO to the PSII core complexes from *T. vulcanus* depleted of all the extrinsic proteins significantly increased an  $O_2$ -evolving activity (43% of the activity of untreated PSII) and lowered the  $Ca^{2+}$  and  $Cl^-$  requirements.<sup>18</sup> It was also observed that the  $\Delta psbO$  mutants of *Synechocystis* sp. PCC 6803 did not grow photoautotrophically at low  $Ca^{2+}$  and  $Cl^-$  concentrations.<sup>62–64</sup> It is thus suggested that the significant recovery of the protein conformation of the OEC by PsbO binding is responsible for the stabilization of the  $Mn_4CaO_5$  cluster by enhancing the  $Ca^{2+}$  and  $Cl^-$  retention capability.

Although the amide I bands of the  $S_2/S_1$  difference spectrum were mostly recovered by PsbO binding, peaks at  $\sim 1670(+)/1662(-)/\sim 1649(+)$   $cm^{-1}$  were commonly left in the double-difference spectra at 5 and 100 mM  $CaCl_2$  (Figure 7c), suggesting that the conformations of a few polypeptide chains are still modified in the absence of other extrinsic proteins. When both PsbV and PsbO bind, the feature was left at  $\sim 1670(+)/1661(-)$   $cm^{-1}$  with a lower intensity (Figure 7d), indicative of further recovery of the protein conformation. An additional signal was observed at 1638 and 1653  $cm^{-1}$  in PsbO-reconstituted and PsbO/V-reconstituted samples, respectively, at 5 mM  $CaCl_2$  (Figure 7c,d, black lines), possibly because of the lower recovery of the conformation at a lower  $CaCl_2$  concentration. When all the PsbO, PsbV, and PsbU proteins bind, the amide I bands, and hence the protein conformation of the OEC, fully recovered (Figure 7e). These recoveries of the protein conformation by the binding of PsbV and PsbU are well correlated with the previous observation of the stepwise recoveries of  $O_2$  evolution activity by PsbV and PsbU (62

and 80%, respectively, of the activity of untreated PSII) in the presence of  $CaCl_2$ .<sup>18</sup> The FTIR results are also consistent with the previous *in vivo* study, in which the  $\Delta psbU$  mutant of *Synechocystis* sp. PCC 6803 showed a minor effect on the OEC functions in comparison with the  $\Delta psbV$  mutant.<sup>65</sup> However, the  $\Delta psbV$  mutant caused a significant alteration such as a lack of growth in the absence of  $Ca^{2+}$  and  $Cl^-$  like that of the  $\Delta psbO$  mutant.<sup>64,65</sup> It could be possible that PsbV has some additional functions *in vivo* in addition to those observed in isolated PSII complexes.

The FTIR results obtained here are summarized in a schematic diagram of the relationship between the OEC conformation and the binding of the extrinsic proteins (Figure 8). Upon depletion of all the extrinsic proteins, the protein

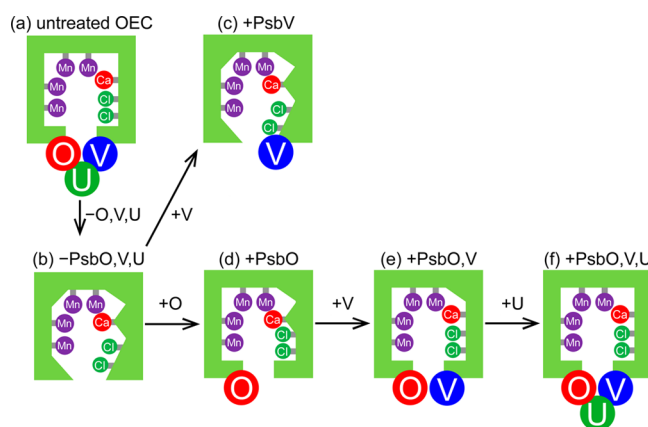


**Figure 8.** Schematic view of the effects of the extrinsic proteins on the protein conformation of the OEC. O, V, and U represent PsbO, PsbV, and PsbU, respectively.

conformation of OEC is significantly altered (Figure 8b). The conformation is significantly recovered upon PsbO binding (Figure 8d), whereas the recovery is not achieved upon single binding of PsbV (Figure 8c). The OEC conformation is further recovered upon binding of PsbO and PsbV (Figure 8e) and fully recovered upon binding of PsbO, PsbV, and PsbU (Figure 8f).

The primary candidates for the polypeptide chains affected by the  $S_1 \rightarrow S_2$  transition are those interacting with the  $Mn_4CaO_5$  cluster and  $Cl^-$  ions via ligation or direct hydrogen bonding. According to the X-ray structure of the PSII core complex of thermophilic cyanobacteria,<sup>7–10</sup> the  $Mn_4CaO_5$  cluster and two  $Cl^-$  ions interact with the C-terminus (D1-Ala344), D1-Asp342, D1-His337, D1-Glu333, and D1-His332 on the C-terminal loop region, D1-Glu189 and D1-Asn181 on the CD helix of the D1 protein, D1-Asp170 on the loop between the CD and C helices of the D1 protein, D2-Lys317 on the C-terminal helical region of the D2 protein, and CP43-Glu354 and CP43-Arg357 on the short  $3_{10}$ -helix of the CP43 protein (Figure 9). The presence of the five polypeptide chains with different secondary structures around the OEC is consistent with the observation of several peaks (1696/1677/1669/1661/1652/1641/1633/1617  $cm^{-1}$ ) in the whole amide I region of 1700–1600  $cm^{-1}$  in the  $S_2/S_1$  difference spectrum of the untreated PSII (Figure 3, black lines). Amide I bands at 1660–1650  $cm^{-1}$  are generally assigned to an  $\alpha$ -helical conformation, while bands around 1665  $cm^{-1}$  could arise from a  $3_{10}$ -helix conformation.<sup>66,67</sup> Although usually  $\beta$ -strands and/or turns have bands at 1640–1620 and 1695–1670

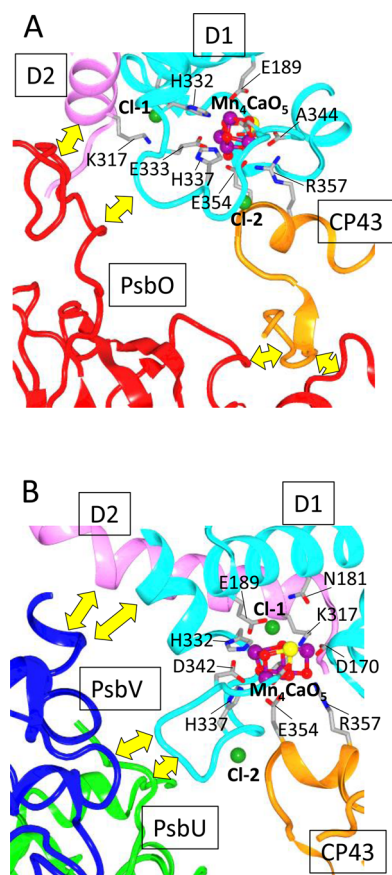


**Figure 9.** Interactions of the extrinsic proteins with the polypeptides forming the OEC in a cyanobacterial PSII core complex: (A) interactions of PsbO and (B) interactions of PsbV and PsbU. Yellow arrows indicate the interaction site. As for the intrinsic proteins, only polypeptide chains directly interacting with the Mn<sub>4</sub>CaO<sub>5</sub> cluster and two Cl<sup>-</sup> ions (Cl-1 and Cl-2) are shown. The coordinates of the high-resolution (1.9 Å) X-ray structure of *T. vulcanus* (Protein Data Bank entry 3ARC<sup>9</sup>) were used.

cm<sup>-1</sup>,<sup>66,67</sup> these conformations are scarcely involved in the polypeptides around the OEC. A nonordered conformation generally shows a band near the region of an  $\alpha$ -helical conformation in H<sub>2</sub>O.<sup>67</sup> However, the loop regions with specific interactions with the Mn<sub>4</sub>CaO<sub>5</sub> cluster and Cl<sup>-</sup> ions via main chain amides and side groups could show irregular amide I frequencies and hence could spread over the whole amide I region.

The X-ray structure (Figure 9A) also shows that PsbO is in direct contact with the C-terminal loop region of the D1 protein between D1-Glu333 and D1-His337 interacting with the Mn<sub>4</sub>CaO<sub>5</sub> cluster, and the C-terminal helix of the D2 protein involving D2-Lys317, a ligand to Cl-1 (the nomenclature of the Cl ions follows that of ref 9). PsbO also interacts with the loop region connected to the short 3<sub>10</sub>-helix of the CP43 protein possessing CP43-Glu354 and CP43-Arg357, which interact with the Mn<sub>4</sub>CaO<sub>5</sub> cluster and provide a ligand to Cl-2 (through the main chain amide of CP43-Glu354). It is notable that there is a short  $\beta$ -strand, which could be the origin of the amide I bands at 1640–1620 and 1695–1670 cm<sup>-1</sup>, between this loop region and the 3<sub>10</sub>-helix. PsbV is also in contact with the C-terminal helix of the D2 protein possessing D2-Lys317, and the C-terminal helix near D1-His332 and the C-terminal loop between D1-Asp342 and D1-

His337 of the D1 protein (Figure 9B). The latter loop region also interacts with the PsbU protein. Thus, these polypeptide chains directly interacting with PsbO, PsbV, and PsbU can be responsible for the amide I peaks at 1679/1672/1663/1651/1643/1633 cm<sup>-1</sup>, which appeared in the double-difference spectrum upon depletion of all the extrinsic proteins (Figure 7a). Because peaks at ~1670/1662/~1649 cm<sup>-1</sup> remained in the double-difference spectrum (Figure 7c) even after PsbO was rebound, these amide I peaks could arise from the polypeptides of the C-terminal helices of the D1 and D2 proteins (for 1662/~1649 cm<sup>-1</sup>) and the C-terminal loop of the D1 protein (for ~1670/1662 cm<sup>-1</sup>), which interact with PsbV and PsbU. This idea is supported by the observation that the signal at ~1670/1662 cm<sup>-1</sup> was left with a decreased intensity when PsbV was further rebound, and hence, only PsbU is depleted (Figure 7d), because PsbU interacts with the same C-terminal loop of the D1 protein (Figure 9B). It is also possible that PsbU, which directly interacts with PsbV (Figure 1), plays a role in strengthening the interaction of PsbV with the D1 protein by stabilizing PsbV binding. PsbV does not have a direct interaction with PsbO and hence can bind to the PSII complex without PsbO. However, PsbV cannot restore the protein conformation by its sole binding, suggesting that the interaction of PsbO probably with the C-terminal loop of the D1 protein is required for the proper interaction of PsbV with the nearby site of the same loop region. Thus, direct interactions of the individual extrinsic proteins with the polypeptide chains around the OEC can well explain the FTIR results of this study. It is, however, noted that because polypeptide chains in the PSII proteins significantly coupled with each other via hydrogen bond networks, indirect interactions between the extrinsic proteins and the polypeptides around the Mn<sub>4</sub>CaO<sub>5</sub> cluster and Cl<sup>-</sup> ions could contribute to the amide I changes in the FTIR spectra.

Cyanobacteria have CyanoP and CyanoQ, which are the homologues of PsbP and PsbQ, respectively, contained in higher plants and green algae.<sup>19,20</sup> Indeed, CyanoQ was identified as one of the components in the isolated PSII complexes from *Synechocystis* sp. PCC 6803<sup>68</sup> and was thought to be involved in the activity and stability of PSII.<sup>21,69</sup> Recently, CyanoQ was also found in purified PSII core complexes from *T. elongatus*.<sup>22</sup> In contrast, CyanoP may not be stoichiometrically involved in PSII complexes<sup>20,22</sup> and was suggested to function during the assembly and/or photoactivation process of PSII.<sup>70</sup> On the other hand, neither CyanoP nor CyanoQ has been found in the crystal structures of PSII core complexes from *T. elongatus*<sup>7,8</sup> and *T. vulcanus*.<sup>9,10</sup> These proteins were also not detected by mass spectrometry in His-tagged PSII core complexes from *T. elongatus* highly purified using Ni affinity chromatography.<sup>71</sup> Our PSII core samples from *T. elongatus* also contained neither CyanoP nor CyanoQ judging from the SDS–PAGE data (Figure 2 and Figure S1 of the Supporting Information). Because the PSII core complexes from *T. elongatus* show high O<sub>2</sub> evolution activity even in the absence of CyanoP and CyanoQ,<sup>71</sup> their contributions to the stability of OEC and O<sub>2</sub> evolution activity seem to be rather minor. Therefore, the conclusion of this study that PsbO significantly contributes to the retention of the protein conformation of the OEC while PsbV and PsbU make minor contributions may hold even when CyanoP and CyanoQ are taken into consideration.

It is generally known that isolated PSII core complexes and their OEC from thermophilic cyanobacteria are more stable

than those from mesophilic cyanobacteria. However, the phenotype of the  $\Delta psbV$  mutant of *T. elongatus*, which lowered the growth rate and  $O_2$  evolution activity,<sup>72</sup> was similar to that of *Synechocystis* sp. PCC 6803.<sup>65</sup> In addition, the effect of depletion of the extrinsic proteins on the stabilization of the  $S_2Q_A^-$  charged pair, which was shown by upshifted peak temperatures in thermoluminescence measurements, was similar between *T. vulcanus* and *Synechocystis*.<sup>18,64,65</sup> Thus, the regulatory roles of the extrinsic proteins in OEC may be similar between thermophilic and mesophilic cyanobacteria.

Our previous FTIR study revealed that the conformation of the OEC in PSII of the red alga *C. caldarium* is regulated mainly by binding of PsbV rather than PsbO.<sup>45</sup> Red algae in the red lineage are thought to have evolved from cyanobacteria and retain PsbO, PsbV, and PsbU with an additional extrinsic protein, PsbQ'. It is interesting that although PsbO was conserved in all oxyphototrophs during evolution, its function was not fully conserved. The function of PsbO in cyanobacteria as a major component for retaining the proper protein conformation of the OEC seemed to be transferred to PsbV in red algae.

As for higher plants, which keep PsbO but have PsbP and PsbQ instead of PsbV and PsbU, our FTIR studies using PSII membranes from spinach have shown that the OEC conformation was mainly regulated by PsbP binding.<sup>42–44,46</sup> It should be noted that although it was recently reported that the removal of PsbP and PsbQ from PSII core preparations of spinach showed no significant effect on the  $S_2/S_1$  spectrum,<sup>73</sup> the control  $S_2/S_1$  spectrum in ref 73 exhibited a typical amide I feature of PsbP-depleted PSII, i.e., lower and higher intensities for the 1668 and 1686  $cm^{-1}$  peaks, respectively (compare the spectrum of Figure 4A in ref 73 with our spectra of Figure 1b in ref 42). Hence, it is suggested that the intact PSII core complexes from spinach in ref 73 were actually depleted of the PsbP and PsbQ proteins when FTIR spectra were measured, possibly because of the presence of potassium ferricyanide in addition to 20 mM  $CaCl_2$ . The latter work also showed that removal of PsbO significantly affected the amide I bands of the  $S_2/S_1$  difference spectrum,<sup>73</sup> whereas our previous measurements showed that PsbO depletion did not induce further changes in the amide I bands of PsbP- and PsbQ-depleted PSII membranes.<sup>42</sup> The latter observation is also consistent with the previous EPR study in which the multiline signal was not affected by the removal of PsbO from spinach PSII membranes.<sup>74</sup> Because experimental conditions are significantly different between our study<sup>42</sup> and ref 73, including the forms of preparations (membranes vs core complexes) and temperatures (250 K vs 263 K), further careful studies will be necessary to reach a conclusion about the contribution of PsbO to the OEC conformation in higher plants.

In conclusion, this FTIR study, by monitoring the changes in the secondary structures of polypeptides upon the  $S_1 \rightarrow S_2$  transition, has shown that PsbO mainly contributes to the retention of the proper protein conformation of the OEC in cyanobacterial PSII. PsbV and PsbU also have some contributions to regulate the OEC conformation by affecting specific polypeptide chains. These conformational changes detected by FTIR are well correlated with the  $O_2$  evolution activity and the  $Ca^{2+}$  and  $Cl^-$  retention capability. Further FTIR studies using PSII samples from different species such as diatoms in the red lineage and green algae in the green lineage will provide a clearer view of the changes in the roles of

extrinsic proteins during the evolution of PSII in oxyphototrophs.

## ■ ASSOCIATED CONTENT

### § Supporting Information

SDS–PAGE analysis of purified extrinsic proteins. This material is available free of charge via the Internet at <http://pubs.acs.org>.

## ■ AUTHOR INFORMATION

### Corresponding Authors

\*Telephone: +81-52-789-2883. Fax: +81-52-789-2883. E-mail: [nagao@bio.phys.nagoya-u.ac.jp](mailto:nagao@bio.phys.nagoya-u.ac.jp).

\*Telephone: +81-52-789-2881. Fax: +81-52-789-2883. E-mail: [tnoguchi@bio.phys.nagoya-u.ac.jp](mailto:tnoguchi@bio.phys.nagoya-u.ac.jp).

### Funding

This study was supported by Grants-in-Aid for Scientific Research from the Ministry of Education, Culture, Sports, Science and Technology (26840091 to R.N., 24370025 and 26220801 to T.T., and 24000018, 24107003, and 25291033 to T.N.).

### Notes

The authors declare no competing financial interest.

## ■ ACKNOWLEDGMENTS

We thank Dr. Hanayo Ueoka-Nakanishi for technical assistance in the preparation of the core complexes of *T. elongatus*.

## ■ ABBREVIATIONS

DM, *n*-dodecyl  $\beta$ -D-maltoside; FTIR, Fourier transform infrared; Mes, 2-(*N*-morpholino)ethanesulfonic acid; PEG6000, polyethylene glycol 6000; PSII, photosystem II.

## ■ REFERENCES

- (1) Debus, R. J. (1992) The manganese and calcium ions of photosynthetic oxygen evolution. *Biochim. Biophys. Acta* 1102, 269–352.
- (2) Hillier, W., and Messinger, J. (2005) Mechanism of photosynthetic oxygen production. In *Photosystem II: The Light-Driven Water:Plastoquinone Oxidoreductase* (Wydrzynski, T. J., and Satoh, K., Eds.) pp 567–608, Springer, Dordrecht, The Netherlands.
- (3) McEvoy, J. P., and Brudvig, G. W. (2006) Water-splitting chemistry of photosystem II. *Chem. Rev.* 106, 4455–4483.
- (4) Messinger, J., Noguchi, T., and Yano, J. (2012) Photosynthetic  $O_2$  evolution. In *Molecular Solar Fuels* (Wydrzynski, T. J., and Hillier, W., Eds.) pp 163–207, Royal Society of Chemistry, Cambridge, U.K.
- (5) Renger, G. (2012) Photosynthetic water splitting: Apparatus and mechanism. In *Photosynthesis: Plastid Biology, Energy Conversion and Carbon Assimilation* (Eaton-Rye, J. J., Tripathy, B. C., and Sharkey, T. D., Eds.) pp 359–414, Springer, Dordrecht, The Netherlands.
- (6) Grundmeier, A., and Dau, H. (2012) Structural models of the manganese complex of photosystem II and mechanistic implications. *Biochim. Biophys. Acta* 1817, 88–105.
- (7) Ferreira, K. N., Iverson, T. M., Maghlaoui, K., Barber, J., and Iwata, S. (2004) Architecture of the photosynthetic oxygen-evolving center. *Science* 303, 1831–1838.
- (8) Guskov, A., Kern, J., Gabdulkhakov, A., Broser, M., Zouni, A., and Saenger, W. (2009) Cyanobacterial photosystem II at 2.9-Å resolution and the role of quinones, lipids, channels and chloride. *Nat. Struct. Mol. Biol.* 16, 334–342.
- (9) Umena, Y., Kawakami, K., Shen, J.-R., and Kamiya, N. (2011) Crystal structure of oxygen-evolving photosystem II at a resolution of 1.9 Å. *Nature* 473, 55–60.
- (10) Suga, M., Akita, F., Hirata, K., Ueno, G., Murakami, H., Nakajima, Y., Shimizu, T., Yamashita, K., Yamamoto, M., Ago, H., et al.

(2015) Native structure of photosystem II at 1.95 Å resolution viewed by femtosecond X-ray pulses. *Nature* 517, 99–103.

(11) De Las Rivas, J., Balsera, M., and Barber, J. (2004) Evolution of oxygenic photosynthesis: Genome-wide analysis of the OEC extrinsic proteins. *Trends Plant Sci.* 9, 18–25.

(12) Roose, J. L., Wegener, K. M., and Pakrasi, H. B. (2007) The extrinsic proteins of Photosystem II. *Photosynth. Res.* 92, 369–387.

(13) Enami, I., Okumura, A., Nagao, R., Suzuki, T., Iwai, M., and Shen, J.-R. (2008) Structures and functions of the extrinsic proteins of photosystem II from different species. *Photosynth. Res.* 98, 349–363.

(14) Fagerlund, R. D., and Eaton-Rye, J. J. (2011) The lipoproteins of cyanobacterial photosystem II. *J. Photochem. Photobiol., B* 104, 191–203.

(15) Ifuku, K., Ido, K., and Sato, F. (2011) Molecular functions of PsbP and PsbQ proteins in the photosystem II supercomplex. *J. Photochem. Photobiol., B* 104, 158–164.

(16) Bricker, T. M., Roose, J. L., Fagerlund, R. D., Frankel, L. K., and Eaton-Rye, J. J. (2012) The extrinsic proteins of Photosystem II. *Biochim. Biophys. Acta* 1817, 121–142.

(17) Falkowski, P. G., Katz, M. E., Knoll, A. H., Quigg, A., Raven, J. A., Schofield, O., and Taylor, F. J. R. (2004) The evolution of modern eukaryotic phytoplankton. *Science* 305, 354–360.

(18) Shen, J.-R., and Inoue, Y. (1993) Binding and functional properties of two new extrinsic components, cytochrome *c*-550 and a 12-kDa protein, in cyanobacterial photosystem II. *Biochemistry* 32, 1825–1832.

(19) Kashino, Y., Lauber, W. M., Carroll, J. A., Wang, Q., Whitmarsh, J., Satoh, K., and Pakrasi, H. B. (2002) Proteomic analysis of a highly active photosystem II preparation from the cyanobacterium *Synechocystis* sp. PCC 6803 reveals the presence of novel polypeptides. *Biochemistry* 41, 8004–8012.

(20) Thornton, L. E., Ohkawa, H., Roose, J. L., Kashino, Y., Keren, N., and Pakrasi, H. B. (2004) Homologs of plant PsbP and PsbQ proteins are necessary for regulation of photosystem II activity in the cyanobacterium *Synechocystis* 6803. *Plant Cell* 16, 2164–2175.

(21) Roose, J. L., Kashino, Y., and Pakrasi, H. B. (2007) The PsbQ protein defines cyanobacterial photosystem II complexes with highest activity and stability. *Proc. Natl. Acad. Sci. U.S.A.* 104, 2548–2553.

(22) Michoux, F., Boehm, M., Bialek, W., Takasaka, K., Maghlaoui, K., Barber, J., Murray, J. W., and Nixon, P. J. (2014) Crystal structure of CyanoQ from the thermophilic cyanobacterium *Thermosynechococcus elongatus* and detection in isolated photosystem II complexes. *Photosynth. Res.* 122, 57–67.

(23) Enami, I., Murayama, H., Ohta, H., Kamo, M., Nakazato, K., and Shen, J.-R. (1995) Isolation and characterization of a Photosystem II complex from the red alga *Cyanidium caldarium*: Association of cytochrome *c*-550 and a 12 kDa protein with the complex. *Biochim. Biophys. Acta* 1232, 208–216.

(24) Enami, I., Kikuchi, S., Fukuda, T., Ohta, H., and Shen, J.-R. (1998) Binding and functional properties of four extrinsic proteins of photosystem II from a red alga, *Cyanidium caldarium*, as studied by release-reconstitution experiments. *Biochemistry* 37, 2787–2793.

(25) Nagao, R., Ishii, A., Tada, O., Suzuki, T., Dohmae, N., Okumura, A., Iwai, M., Takahashi, T., Kashino, Y., and Enami, I. (2007) Isolation and characterization of oxygen-evolving thylakoid membranes and Photosystem II particles from a marine diatom *Chaetoceros gracilis*. *Photosynth. Res.* 1767, 1353–1362.

(26) Nagao, R., Tomo, T., Noguchi, E., Nakajima, S., Suzuki, T., Okumura, A., Kashino, Y., Mimuro, M., Ikeuchi, M., and Enami, I. (2010) Purification and characterization of a stable oxygen-evolving Photosystem II complex from a marine centric diatom, *Chaetoceros gracilis*. *Biochim. Biophys. Acta* 1797, 160–166.

(27) Nagao, R., Moriguchi, A., Tomo, T., Niikura, A., Nakajima, S., Suzuki, T., Okumura, A., Iwai, M., Shen, J.-R., Ikeuchi, M., et al. (2010) Binding and functional properties of five extrinsic proteins in oxygen-evolving photosystem II from a marine centric diatom, *Chaetoceros gracilis*. *J. Biol. Chem.* 285, 29191–29199.

(28) Nagao, R., Suga, M., Niikura, A., Okumura, A., Koua, F. H. M., Suzuki, T., Tomo, T., Enami, I., and Shen, J.-R. (2013) Crystal

structure of Psb31, a novel extrinsic protein of photosystem II from a marine centric diatom and implications for its binding and function. *Biochemistry* 52, 6646–6652.

(29) Miyao, M., and Murata, N. (1989) The mode of binding of three extrinsic proteins of 33 kDa, 23 kDa and 18 kDa in photosystem II complex of spinach. *Biochim. Biophys. Acta* 977, 315–321.

(30) Suzuki, T., Minagawa, J., Tomo, T., Sonoike, K., Ohta, H., and Enami, I. (2003) Binding and functional properties of the extrinsic proteins in oxygen-evolving photosystem II particle from a green alga, *Chlamydomonas reinhardtii* having his-tagged CP47. *Plant Cell Physiol.* 44, 76–84.

(31) Ifuku, K. (2014) The PsbP and PsbQ family proteins in the photosynthetic machinery of chloroplasts. *Plant Physiol. Biochem.* 81, 108–114.

(32) Chu, H.-A., Hillier, W., Law, N. A., and Babcock, G. T. (2001) Vibrational spectroscopy of the oxygen-evolving complex and of manganese model compounds. *Biochim. Biophys. Acta* 1503, 69–82.

(33) Noguchi, T., and Berthomieu, C. (2005) Molecular analysis by vibrational spectroscopy. In *Photosystem II: The Light-Driven Water-Plastoquinone Oxidoreductase* (Wydrzynski, T. J., and Satoh, K., Eds.) pp 367–387, Springer, Dordrecht, The Netherlands.

(34) Noguchi, T. (2007) Light-induced FTIR difference spectroscopy as a powerful tool toward understanding the molecular mechanism of photosynthetic oxygen evolution. *Photosynth. Res.* 91, 59–69.

(35) Debus, R. J. (2008) Protein ligation of the photosynthetic oxygen-evolving center. *Coord. Chem. Rev.* 252, 244–258.

(36) Noguchi, T. (2008) Fourier transform infrared analysis of the photosynthetic oxygen-evolving center. *Coord. Chem. Rev.* 252, 336–346.

(37) Noguchi, T. (2008) FTIR detection of water reactions in the oxygen-evolving center of photosystem II. *Philos. Trans. R. Soc., B* 363, 1189–1195.

(38) Chu, H.-A. (2013) Fourier transform infrared difference spectroscopy for studying the molecular mechanism of photosynthetic water oxidation. *Front. Plant Sci.* 4, 146.

(39) Noguchi, T. (2013) Monitoring the reactions of photosynthetic water oxidation using infrared spectroscopy. *Biomed. Spectrosc. Imaging* 2, 115–128.

(40) Debus, R. J. (2015) FTIR studies of metal ligands, networks of hydrogen bonds, and water molecules near the active site Mn<sub>4</sub>CaO<sub>5</sub> cluster in Photosystem II. *Biochim. Biophys. Acta* 1847, 19–34.

(41) Noguchi, T. (2015) Fourier transform infrared difference and time-resolved infrared detection of the electron and proton transfer dynamics in photosynthetic water oxidation. *Biochim. Biophys. Acta* 1847, 35–45.

(42) Tomita, M., Ifuku, K., Sato, F., and Noguchi, T. (2009) FTIR evidence that the PsbP extrinsic protein induces protein conformational changes around the oxygen-evolving Mn cluster in photosystem II. *Biochemistry* 48, 6318–6325.

(43) Ido, K., Kakiuchi, S., Uno, C., Nishimura, T., Fukao, Y., Noguchi, T., Sato, F., and Ifuku, K. (2012) The conserved His-144 in the PsbP protein is important for the interaction between the PsbP N-terminus and the Cyt *b*<sub>559</sub> subunit of photosystem II. *J. Biol. Chem.* 287, 26377–26387.

(44) Kakiuchi, S., Uno, C., Ido, K., Nishimura, T., Noguchi, T., Ifuku, K., and Sato, F. (2012) The PsbQ protein stabilizes the functional binding of the PsbP protein to photosystem II in higher plants. *Biochim. Biophys. Acta* 1817, 1346–1351.

(45) Uno, C., Nagao, R., Suzuki, H., Tomo, T., and Noguchi, T. (2013) Structural coupling of extrinsic proteins with the oxygen-evolving center in red algal photosystem II as revealed by light-induced FTIR difference spectroscopy. *Biochemistry* 52, 5705–5707.

(46) Nishimura, T., Uno, C., Ido, K., Nagao, R., Noguchi, T., Sato, F., and Ifuku, K. (2014) Identification of the basic amino acid residues on the PsbP protein involved in the electrostatic interaction with photosystem II. *Biochim. Biophys. Acta* 1837, 1447–1453.

(47) Iwai, M., Suzuki, T., Kamiyama, A., Sakurai, I., Dohmae, N., Inoue, Y., and Ikeuchi, M. (2010) The PsbK subunit is required for the stable assembly and stability of other small subunits in the PSII

complex in the thermophilic cyanobacterium *Thermosynechococcus elongatus* BP-1. *Plant Cell Physiol.* 51, 554–560.

(48) Nakamura, S., Nagao, R., Takahashi, R., and Noguchi, T. (2014) Fourier transform infrared detection of a polarizable proton trapped between photooxidized tyrosine Yz and a coupled histidine in photosystem II: Relevance to the proton transfer mechanism of water oxidation. *Biochemistry* 53, 3131–3144.

(49) Noguchi, T., and Inoue, Y. (1995) Identification of Fourier transform infrared signals from the non-heme iron in photosystem II. *J. Biochem.* 118, 9–12.

(50) Suzuki, H., Taguchi, Y., Sugiura, M., Boussac, A., and Noguchi, T. (2006) Structural perturbation of the carboxylate ligands to the manganese cluster upon  $\text{Ca}^{2+}/\text{Sr}^{2+}$  exchange in the S-state cycle of photosynthetic oxygen evolution as studied by flash-induced FTIR difference spectroscopy. *Biochemistry* 45, 13454–13464.

(51) Noguchi, T., and Sugiura, M. (2000) Structure of an active water molecule in the water-oxidizing complex of photosystem II as studied by FTIR spectroscopy. *Biochemistry* 39, 10943–10949.

(52) Noguchi, T., and Sugiura, M. (2001) Flash-induced fourier transform infrared detection of the structural changes during the S-state cycle of the oxygen-evolving complex in photosystem II. *Biochemistry* 40, 1497–1502.

(53) Noguchi, T., and Sugiura, M. (2002) Flash-induced FTIR difference spectra of the water oxidizing complex in moderately hydrated photosystem II core films: Effect of hydration extent on S-state transitions. *Biochemistry* 41, 2322–2330.

(54) Noguchi, T., and Sugiura, M. (2002) FTIR detection of water reactions during the flash-induced S-state cycle of the photosynthetic water-oxidizing complex. *Biochemistry* 41, 15706–15712.

(55) Noguchi, T., and Sugiura, M. (2003) Analysis of flash-induced FTIR difference spectra of the S-state cycle in the photosynthetic water-oxidizing complex by uniform  $^{15}\text{N}$  and  $^{13}\text{C}$  isotope labeling. *Biochemistry* 42, 6035–6042.

(56) Kimura, Y., Mizusawa, N., Ishii, A., Yamanari, T., and Ono, T. (2003) Changes of low-frequency vibrational modes induced by universal  $^{15}\text{N}$ - and  $^{13}\text{C}$ -isotope labeling in  $\text{S}_2/\text{S}_1$  FTIR difference spectrum of oxygen-evolving complex. *Biochemistry* 42, 13170–13177.

(57) Noguchi, T., Ono, T., and Inoue, Y. (1995) Direct detection of a carboxylate bridge between Mn and  $\text{Ca}^{2+}$  in the photosynthetic oxygen-evolving center by means of Fourier transform infrared spectroscopy. *Biochim. Biophys. Acta* 1228, 189–200.

(58) Chu, H.-A., Hillier, W., and Debus, R. J. (2004) Evidence that the C-terminus of the D1 polypeptide of photosystem II is ligated to the manganese ion that undergoes oxidation during the  $\text{S}_1$  to  $\text{S}_2$  transition: An isotope-edited FTIR study. *Biochemistry* 43, 3152–3166.

(59) Shimada, Y., Suzuki, H., Tsuchiya, T., Tomo, T., Noguchi, T., and Mimuro, M. (2009) Effect of a single-amino acid substitution of the 43 kDa chlorophyll protein on the oxygen-evolving reaction of the cyanobacterium *Synechocystis* sp. PCC 6803: Analysis of the Glu354Gln mutation. *Biochemistry* 48, 6095–6103.

(60) Service, R. J., Yano, J., McConnell, I., Hwang, H. J., Nicks, D., Hille, R., Wydrzynski, T., Burnap, R. L., Hillier, W., and Debus, R. J. (2011) Participation of glutamate-354 of the CP43 polypeptide in the ligation of manganese and the binding of substrate water in photosystem II. *Biochemistry* 50, 63–81.

(61) Enami, I., Yoshihara, S., Tohri, A., Okumura, A., Ohta, H., and Shen, J.-R. (2000) Cross-reconstitution of various extrinsic proteins and photosystem II complexes from cyanobacteria, red algae and higher plants. *Plant Cell Physiol.* 41, 1354–1364.

(62) Burnap, R. L., and Sherman, L. A. (1991) Deletion mutagenesis in *Synechocystis* sp. PCC6803 indicates that the Mn-stabilizing protein of photosystem II is not essential for  $\text{O}_2$  evolution. *Biochemistry* 30, 440–446.

(63) Philbrick, J. B., Diner, B. A., and Zilinskas, B. A. (1991) Construction and characterization of cyanobacterial mutants lacking the manganese-stabilizing polypeptide of photosystem II. *J. Biol. Chem.* 266, 13370–13376.

(64) Burnap, R. L., Shen, J.-R., Jursinic, P. A., Inoue, Y., and Sherman, L. A. (1992) Oxygen yield and thermoluminescence characteristics of a

cyanobacterium lacking the manganese-stabilizing protein of photosystem II. *Biochemistry* 31, 7404–7410.

(65) Shen, J.-R., Qian, M., Inoue, Y., and Burnap, R. L. (1998) Functional characterization of *Synechocystis* sp. PCC 6803  $\Delta\text{psbU}$  and  $\Delta\text{psbV}$  mutants reveals important roles of cytochrome  $c$ -550 in cyanobacterial oxygen evolution. *Biochemistry* 37, 1551–1558.

(66) Byler, D. M., and Susi, H. (1986) Examination of the secondary structure of proteins by deconvolved FTIR spectra. *Biopolymers* 25, 469–487.

(67) Surewicz, W. K., and Mantsch, H. H. (1988) New insight into protein secondary structure from resolution-enhanced infrared spectra. *Biochim. Biophys. Acta* 952, 115–130.

(68) Liu, H., Zhang, H., Weisz, D. A., Vidavsky, I., Gross, M. L., and Pakrasi, H. B. (2014) MS-based cross-linking analysis reveals the location of the PsbQ protein in cyanobacterial photosystem II. *Proc. Natl. Acad. Sci. U.S.A.* 111, 4638–4643.

(69) Kashino, Y., Inoue-Kashino, N., Roose, J. L., and Pakrasi, H. B. (2006) Absence of the PsbQ protein results in destabilization of the PsbV protein and decreased oxygen evolution activity in cyanobacterial photosystem II. *J. Biol. Chem.* 281, 20834–20841.

(70) Cormann, K. U., Bartsch, M., Rögner, M., and Nowaczyk, M. M. (2014) Localization of the CyanoP binding site on photosystem II by surface plasmon resonance spectroscopy. *Front. Plant Sci.* 5, 595.

(71) Sugiura, M., Iwai, E., Hayashi, H., and Boussac, A. (2010) Differences in the interactions between the subunits of photosystem II dependent on D1 protein variants in the thermophilic cyanobacterium *Thermosynechococcus elongatus*. *J. Biol. Chem.* 285, 30008–30018.

(72) Katoh, H., Itoh, S., Shen, J.-R., and Ikeuchi, M. (2001) Functional analysis of *psbV* and a novel c-type cytochrome gene *psbV2* of the thermophilic cyanobacterium *Thermosynechococcus elongatus* strain BP-1. *Plant Cell Physiol.* 42, 599–607.

(73) Offenbacher, A. R., Polander, B. C., and Barry, B. A. (2013) An intrinsically disordered photosystem II subunit, PsbO, provides a structural template and a sensor of the hydrogen-bonding network in photosynthetic water oxidation. *J. Biol. Chem.* 288, 29056–29068.

(74) Miller, A.-F., De Paula, J. C., and Brudvig, G. W. (1987) Formation of the  $\text{S}_2$  state and structure of the Mn complex in photosystem II lacking the extrinsic 33 kDa polypeptide. *Photosynth. Res.* 12, 205–218.